ANALYSIS OF CLAW POLE TRANSVERSE FLUX INDUCTOR MOTOR BY MEANS OF MAGNETIC EQUIVALENT CIRCUIT

Dr. SAAD EL-DRIENY

Electrical Engineering Department, Faculty of Engineering,
EL-Mansoura University, EL-Mansoura,
EGYPT

ملخص البحث

تحليل المجال المغناطيس لمحرك الفيض المغناطيسى المتعامد ذو الاقطاب المختلفة التجانس بشكل صعوبة بالغة نظرا لتعدد المسارات للمجال المغناطيسى المتعامد ـ فى هذة الحالة يلزم زيادة القوة الدافعة المغناطيسية للاثارة الناشئة مما يدفع الدائرة المغناطيسية للوصول الى حالة التشبع ، مما يلزم زيادة وزن المحرك لتجنب حدوث هذا التشبع ، يقوم البحث بتحليل المجال المغناطيسى لهذا المحرك بنظام "الدائرة المكافئة المغناطيسية" وبتم قسمة حساب المعاوقة المغناطيسية بفرض مسارات خطية ودائرية للمجال المغناطيسى المستقاد والمتعامد بأنواعة وتوصيلهما بمصادر القوة الدافعة المغناطيسية طبقا لاتجاة المجالات المغناطيسية المتناظرة ، ولقد تم حساب المجال المتعامد وكثافة الفيض المغناطيسى للاقطاب والقوة الدافعة الكهربائية المتولدة فى ملفات التيار المتردد عند وجود ماثة أمبير لفة ناشئة عن ملفات التيار المستمر وكذلك تم حساب المعاوقة المباشرة والمتعامدة للوحة (X_d and X_q) لملفات التيار المتردد وذلك فى حالة وجود ماثة أمبير لفة ناشئة عن تلك الملفات.

ولقد اجريت التجارب المعملية على نموزج استاتيكى للمحرك فى المعمل لتأكيد سلامة تطبيق طريقة الدائرة المكافئة المغناطيسية لمثل هذا النوع من المحركات حيث تقاربت كل من النتائج الحاسبة والمعملية فى الحالة النموذجية حيث المحرك معزول مغناطيسيا عن هيكل التثبيت ، ويفتح هذا الاسلوب لحساب الدائرة المغناطيسية طريقا مبسطا يمكن الاعتماد علية لحساب تصميم وأداء هذا المحرك.

ABSTRACT

In a preliminary design stage of claw pole transverse flux inductor motor with E-core, an accurate magnetic calculations are very complicated due to the field arrangement. A special heavy burden is the estimation of leakage flux in the non-useful paths. Extra iron will be needed to carry this flux if saturation is to be avoided in the useful paths.

This paper presents a simple equivalent circuit method by which the performance of various magnetic paths are estimated analytically. The method is based on the assumption that the flux paths are made up of straight and circular segments. It can be simply and quickly applied to examine the effects of varying the major dimensions of the motor. Experimental measurments are carried out on a simple static model to verify the proposed method. The comparison between the analytical results obtained from an ideal motor and the experimental results shows that they are in better agreement.

LIST OF SYMBLOS

a : = the distance between the out-side limb and centre limb
A : = intermediate expression
b : = out-side limb width
B : = intermediate expression
c : = pole depth including the air-gap length
d : = pole width
e : = induced e.m.f. , r.m.s.
f : = frequency
F_F : = mmf of field winding per one side

g : = air-gap length
g : = effective air-gap length inclusive Carter's coefficient
K_w: = fundamental winding factor
$\hat{F}_a$: = the peak value of resultant armature mmf distribution
N_{ph}: = number of turns per phase
N_f: = number of turns per one side of field winding
p : = pole pitch
S : = permeance
w : = centre-core width
ϕ : = flux
μ_o: = permeability of free space

SUBSCRIPTS

These subscripts denoting the permeances

1 : = outer gap , 4 : = pole to pole leakage
2 : = centre gap , 5 : = pole to ground leakage
3 : = transverse leakage , 6 : = equivalent pole leakage

1. INTRODUCTION

In the early design stages of claw pole transverse flux inductor motor, it is always required to have a quick and handly simple tool to analyse the relevant magnetic circuit and examine the effects of varying the major dimensions of the machine. Consequently, a preliminary estimation of the motor performance can be obtained. Levi [1] had applied a technique which is based on the use of conformal mapping [2], for getting the 2-dimensional plot of the field lines, by means of the Schwartz - Christroffel transformation coupled with numerical integration. Eastham [3] had used a magnetic equivalent circuit assuming that all flux components cross the air-gap in a direction normal to the stator surface. To account for fringing effects, effective pole widths were used by applying Carter's Coefficients. This magnetic equivalent circuit does not consider for leakage flux which is an inherent nature of this motor. This leakage flux affects the machine performance as well as dimensions which must be chosen properly when magnetic saturation is to be avoided.

In this paper a simple magnetic equivalent circuit of the mentioned motor, see figure (1), has been suggested. This circuit takes into consideration the most possible leakage fluxes. Permeance calculations is based on the assumption that the paths of the flux components are made up of straight and circular segments. The configuration of the proposed circuit can be reduced to represent one pole. To get its parameters, represented by the permeances of the propable paths of the different flux components, the permeability of the iron is assumed to be infinity. Special considerations are necessary when dealing with the proposed magnetic equivalent circuit owing to the unorthdox shape of the motor structure.

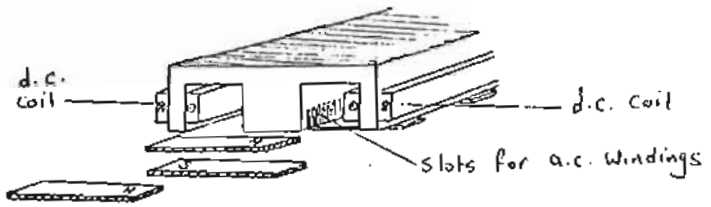

Figure 1 : Claw pole transverse flux inductor motor

2- MAGNETIC EQUIVALENT CIRCUIT

The magnetic field in the air gap region of the motor under investigations, behaves in a complex manner in all three dimensions. The principle flux paths are shown in figure (2), which illustrates the path of the useful flux ϕ_2, which links the armature winding on the central slotted portion of the core. In addition, the outer paths are of the leakage flux components, which contribute to the total flux linking the field winding. Leakage flux emerging from the sides limbs of the core is naturally existing but is not considered in the magnetic model. Also, the iron paths are assumed to have infinite permeability. The flux paths in air are simulated by their permeances and connected in the magnetic equivalent circuit according to their starting and end points. Figure (3a) shows the magnetic circuit analogue for two poles of the machine. This circuit can be simplified by symmetry arguments to be equivalent for one pole : the element S_4, connecting north and south poles of equal and opposite potential, can be severed and connecting the severed ends to earth, hence the poles of the machine are separated The element S_5, is now in parallel with the two severed elements of S_4 to form a total permeance S_6, which connects the pole to earth:

$$S_6 = 4\,S_4 + S_5 \qquad \ldots(1)$$

The magnetic equivalent circuit per pole Figure (3b), can be solved to get the pole magnetic potential F_p, interms the total field m.m.f, F_F :

$$F_p = \frac{S_1 - S_3}{S_1 + S_2 + S_3 + 4S_4 + S_5} \cdot F_F \qquad \ldots(2)$$

Consequently, the pole flux $\phi_1 = (F_F - F_p)S_1$ $\qquad \ldots(3)$

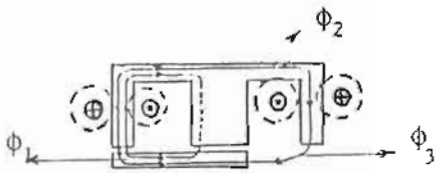

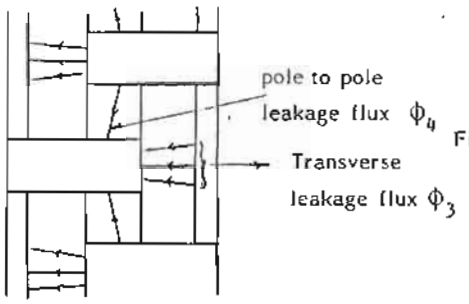

Fig. (2) : Principal flux paths

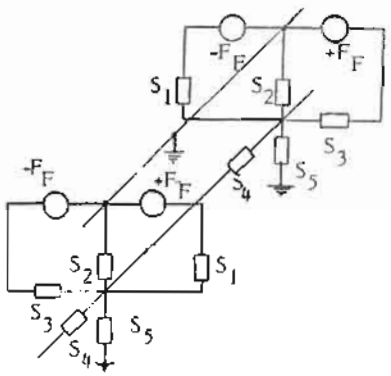

Fig. (3a) : Equivalent circuit for two poles of the machine

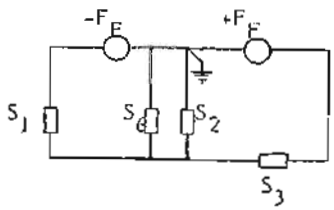

Fig. (3b) : Simplified equivalent circuit for one pole

Accordingly, the useful flux (through the middle limb) and the different components of the leakage flux can be determined as followings:

Useful flux $\phi_2 = F_p . S_2$ ... (4)

Transverse leakage flux $\phi_3 = (F_F + F_p) . S_3$ ... (5)

Pole to pole leakage flux $\phi_4 = 2F_p . S_4$ ... (6)

Pole to ground leakage flux $\phi_5 = F_p . S_4$ ... (7)

The usefulness of the magnetic equivalent circuit depends entirely on the accuracy with which the values of the equivalent circuit elements can be calculated. This is not simple in a case where uniform fields are not common. The fringes of air-gaps, in many cases, carry as much flux as the region directly inside the air-gaps. In paths crossing large gaps the flux lines are assumed to be made up of a combination of straight and circular lines. The paths defined are only an approximation to the actual path and are likely to underestimate the permeance of a path since the actual path is a condition of maximum permeance. It follows now the determinations of the permeances of the different paths:

2-1 Permeances of out side-gap S_1, and Centre-gap S_2

To get S_1 the corresponding flux paths are assumed to follow circular fringes outside the gap as indicated in figure (4). In accordance with S_2, the division of the centre gap is similar, see figure (5), but the air-gap, g, is multiplied by Carter's coefficient to allow for the slotting of the stator.

The fluxes carrying region can be divided into seven individual regions possessing the following permeances :

Out-side gap S_1	Centre-gap S_2
$s_1 = \mu_o\, b\, d / g$	$s'_1 = \mu_o\, w\, d / g'$
$s_2 = 0.61\, \mu_o\, d$	$s'_2 = 0.61\, \mu_o\, d$
$s_3 = 0.305\, \mu_o d$	$s'_3 = 0.305\, \mu_o\, d$
$s_4 = (\mu_o\, d/\pi) \ln (1+2h/g)$	$s'_4 = (\mu_o\, d/\pi) \ln (1+2h/g')$
$s_5 = (2\, \mu_o\, d/\pi) \ln (1+h/g)$	$s'_5 = (2\, \mu_o\, d/\pi) \ln (1+ h/g')$
$s_6 = 0.61\ \mu_o\, b$	$s'_6 = 0.61\ \mu_o\, w$
$s_7 = (2\, \mu_o b\, /\pi) \ln (1+h\, /g)$	$s'_7 = (2\, \mu_o\, w\, /\pi) \ln (1+ h/g')$
$S_1 = s_1 + s_2 + s_3 + s_4 + s_5 + 2 (s_6 + s_7)$ ... (8)	$S_2 = s'_1 + s'_2 + s'_3 + s'_4 + s'_5 + 2 (s'_6 + s'_7)$ ... (9)

2.2 Permeance of transverse leakage path S_3

This permeance can be calculated by the following formula according to the detailed derivation given in the appendix .

$$S_3 = \mu_o \left(\frac{J}{A} \ln \left(1 + \frac{A\, b}{B} \right) + \frac{c}{B} \right) \quad \ldots (10)$$

where :

where ;

$$A = \left(\frac{\pi}{2} + \gamma\right) / d + \left(\frac{\pi}{2} - \gamma\right) / (2p - d) \qquad \ldots (11)$$

$$B = \frac{\sqrt{a^2 + c^2}}{2(p-d)} \ln\left(\frac{2p}{d} - 1\right) \qquad \ldots (12)$$

$$\gamma = \tan^{-1}(c/a) \qquad \ldots (13)$$

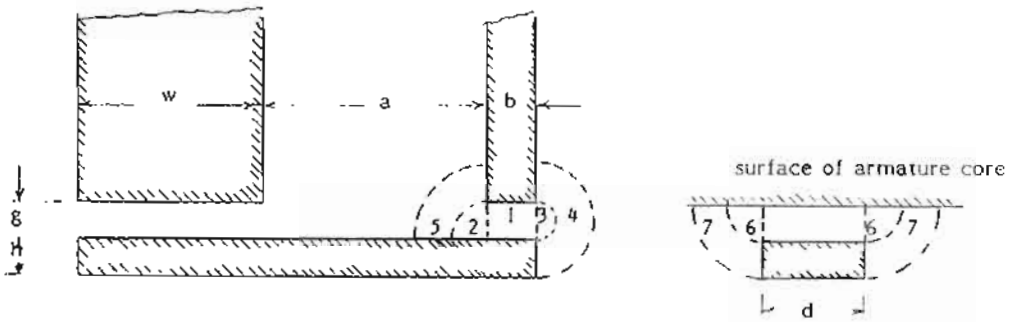

Fig. (4) : Division of side air-gap into component flux paths

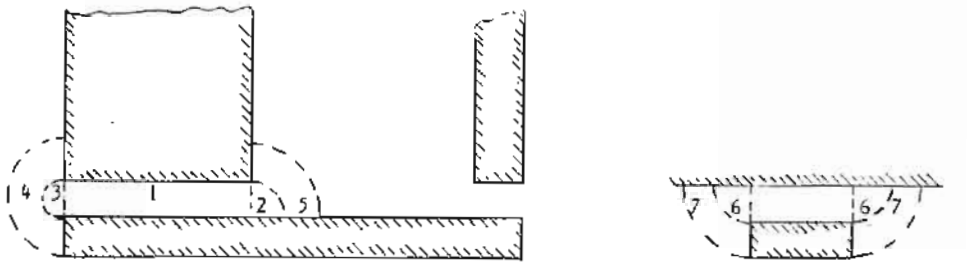

Fig. (5) : Division of centre air-gap into component flux paths

2.3 Permeance of pole to pole leakage path S_4

The corresponding individual paths are shown in Figure (6), and accordingly the whole region can be divided into four individual regions possessing the following peremeances :-

$$s_1 = \mu_o \frac{w-d}{p-d}$$

$$s_2 = 1.22\ \mu_o\ d$$

$$s_3 = \frac{4\mu_o d}{\pi} \ln\left(1 + \frac{d/2}{p-d}\right)$$

$$s_4 = \mu_o \frac{w}{\pi} \ln\left(1 + \frac{d}{p-d}\right)$$

Consequently, the permeance S_4 is the sum of all the above four individual permeances

$$S_4 = \mu_o\, d\, [\ (w-d)/(p-d) + 1.22 + (4/\pi)\cdot \ln(1 + d/(2(p-d)))] + (\mu_o\, w/\pi)\cdot \ln(1 + (d/(p-d))) \quad \ldots (14)$$

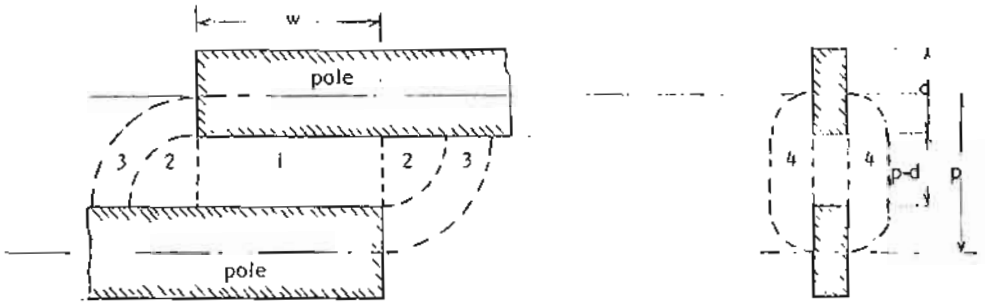

Fig. (6) : Division of pole to pole leakage into component flux paths

2.4 Permeance of pole to ground leakage path S_5

This permeance is calculated simply by taking A_p as the cross section area of the bolt fixing the pole to iron structure and l_o is the length of this bolt, thus

$$S_5 = \mu_o\, A_p / l_o \quad \ldots (15)$$

3- PREDICTION OF SYNCHRONOUS REACTANCES

The flux created by the armature winding is divided into two flux components in both direct and quadrature axes. The direct-axis armature field takes transverse paths [4] as the main field created by the direct current excitation, see figure (7). So, the same technique used to predict the behaviour of the main field can be also used to predict the behaviour of the direct-axis armature field. This can be analysed using a magnetic equivalent circuit, see figure (8), similar to that of the direct current excitation, figure (3), with a slight differenc. This difference is due to the existance of the a.c. excitation on the centre limb of the core.

As the a.c. winding is distributed one, the corresponding source of mmf is distributed sinusoidally along the direction of the machine length. The equivalent mmf in the direct-axis which is appearing across this source on open circuit, F_{od} ,is calculated by summing the flux contributions from each element under the centre air-gap as followings:-

Since the direct-axis mmf component of armature mmf at any point x from the centre pole along the machine length, assuming unity power factor, [5] is given as :-

$$F_{ad} = \hat{F}_a \cos(\pi . x / p) \qquad 0 \leq x \leq p \quad \ldots (16)$$

whereas the flux entres the pole equal to the flux reappears from it, therefore the total flux in the centre air-gap within the pole width must be zero hence,

$$d\phi = 0 = (\mu_o\, w/g) \int_{-d/2}^{d/2} (\hat{F}_a \cos(\pi x/p) - F_{od})\, . \, dx \quad \ldots (17)$$

Then

$$F_{od} = \hat{F}_a\, (2p/(\pi . d))\, \sin(\pi d/2p) \quad \ldots (18)$$

From figure (8) the expression of pole potential F_p can be obtained interms of the direct- axis equivalent mmf, F_{od}, and the parameters S_1, S_2, S_3, S_6 as following :-

$$F_p = \frac{S_2}{S_1 + S_2 + S_3 + S_6} F_{od} \qquad (19)$$

Consequently, the following expressions for the fluxes can be obtained:-

Transverse leakage flux $\Phi_3 = F_p \cdot S_3$ (20)

pole to pole leakage flux $\Phi_4 = F_p \cdot S_6$ (21)

pole flux $\Phi_1 = F_p \cdot S_1$ (22)

centre air-gap flux , or $\Phi_2 = (F_{od} - F_p) S_2$ (23)

(component of the direct-axis armature flux Φ_{ad})
The source permeance is given by the integral of all the elemental parallel paths, ds, then;

$$S_2 = \int_{-d/2}^{d/2} \frac{\mu_o w}{g`} dx = \frac{\mu_o w d}{g`} \qquad (24)$$

once the equation (23) has been solved, the fundamental component of the centre limb air-gap flux density can be obtained. Finally equating the expressions for the induced emf, E_{ad} and the air-gap direct reactance voltage drop $X_d \cdot I_{ad}$ for 100 peak of resultant armature mmf, the armature direct reactance can be obtained.

$$X_d = \frac{4.44 \Phi_2 f N_{ph} K_w}{I_{ad}} \qquad (25)$$

where I_{ad} is the d-axis component of the armature current.

The quadrature-axis field takes longitudinal paths [4], see figure (9). Therefore this flux component demands quite a different treatmeant. Flux tends to emerge from the points on the armature winding at highest potential and these are furthest from the poles. This flux entres the pole near the leading edge and reappears from the trailing edge. The paths are almost entirely axial. Figure (9) shows this occuring and figure (10) shows how the region can be divided into segments for the purpose of calculation. The fluxes are calculated as followings :-

Since the quadrature-axis mmf component of armature mmf at any point x from the centre pole along the machine length is given as [5] :

$$F_{aq}(x) = \hat{F}_a \sin(\pi x / p) \qquad 0 \leqslant x \leqslant p \qquad (26)$$

hence,

$$\phi_{q1} = \frac{\mu_o w}{g} \hat{F}_a \int_0^{x_1} \sin \frac{\pi x}{p} \, dx \quad ; \qquad \ldots (27)$$

$$\phi_{q2} = \frac{\mu_o w}{g} \hat{F}_a \int_{x_1}^{x_2} \sin \frac{\pi x}{p} \, dx \quad ; \qquad \ldots (28)$$

$$\phi_{q3} = \frac{\mu_o w}{g} \hat{F}_a \int_{x_3}^{x_4} \frac{\sin \pi x / p}{(\pi/2)(x - x_1)} \, dx \quad ; \qquad \ldots (29)$$

$$\phi_{q4} = \frac{\mu_o w}{g} \hat{F}_a \int_{x_4}^{p/2} \frac{\sin \pi x / p}{(\pi/2)(2x - x_1 - x_4)} \, dx \qquad \ldots (30)$$

The last two integrals cannot be evaluated directly and a numerical method must be used to evaluate them :
The quadrature axis flux ϕ_{aq} is given as

$$\phi_{aq} = 2 (\phi_{q1} + \phi_{q2} + \phi_{q3} + \phi_{q4}) \qquad \ldots (31)$$

Equating the expressions for the induced emf, E_{aq}, and the air-gap quadrature reactance voltage drop $X_q I_{aq}$, for 100 peak of resultant armature mmf, the armature quadrature reactance can be obtained :

$$X_q = \frac{4.44 \phi_{aq} f . N_{ph} K_w}{I_{aq}} \qquad \ldots (32)$$

where I_{aq} is the q-axis component of the armature current

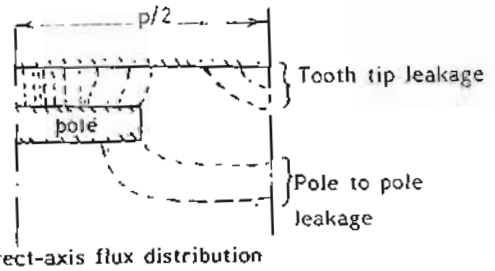

Fig. (7) : Direct-axis flux distribution

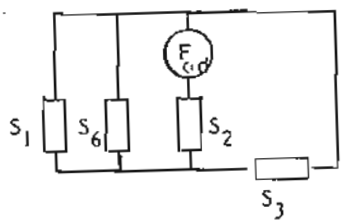

Fig. (8) : Direct-axis field equivalent circuit

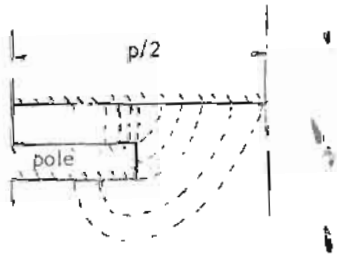

Fig. (9) : Quadrature axis flux distribution

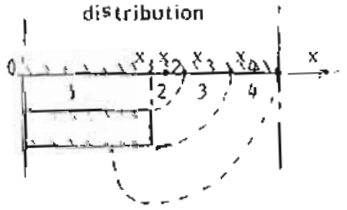

Fig. (10) : Flux paths assumed

4-NUMERICAL EXAMPLE AND EXPERIMENTAL RESULTS

A numerical example is carried out for a static model of the motor which is built in the electric machine laboratory of EL-Mansoura University . The model is made of mild steel sections with a laminated and wound centre core. The D.C. coils are positioned on the outer side limbs of the armature core , one coil at each side. The armature windings are 3-phase with 2 slot/pole/phase and double layer windings. The poles are made of solid mild steel and have a rectangular shape.The D.C. coils are excited from the D.C. supply and the induced emf is measured across the armature winding per phase.

The model has the following data :
outer limb width, b = 35 mm
centre limb width, w = 100 mm
pole depth, h = 20 mm
the distance between the centre limb, and the outer side limb, a =115 mm
overall width 400 mm
air-gap depth, g = 20 mm
pole width, d = 80 mm
pole pitch, p = 180 mm
number of poles = 6
stator back iron thickness = 25 mm
stator stack height = 60 mm
N_f = 200 number of turns of direct current field windings per one side
N_{ph} = 468 number of turns of armature a.c. windings per phase

The fluxes calculated are :-
Φ_1 :the pole flux

Φ_2 : the useful flux or the centre limb flux

Φ_3 : the transverse leakage flux

Φ_4 : the pole to pole leakage flux

The open circuit induced emf in the armature winding due to the excitation of the D.C. winding can be predicted from the value of Φ_2 , the main useful flux linking the armature winding , for 1 Amp. field winding current, the induced emf per phase is given by :-

$$e = 4.44\ K_w\ .f.\ N_{ph}.\ \Phi_2\ .\ (N_f/100)$$

This is calculated and is shown in table (1) . Also , this can be measured experimently at low field excitation for comparison with the predicted one and it is shown in brackets in table (1). The last raw shows the expected values of flux density in the pole for 20 Amp. excitation and it is still unsaturated. From table (1) it can be seen that the transverse leakage flux is quite large even its path has a relatively low permeance. This is because of large difference in magnetic potential between the pole and the opposite side limb (F_p-(-F_F)). The potential difference across this element is 4 to 6 times that across the centre gap. This table shows clearly the difference in amounts of leakage fluxes. The leakage factor of the track pole is defined as the ratio of the total pole flux, Φ_1 ,to the useful flux, Φ_2 . Table (2) shows the pole potential and armature flux component in d-axis for 100 armature mmf, also shows the direct-axis reactance. It shows also, the components of contributions fluxes in case of q-axis armature flux due to 100 armature mmf , the armature flux component Φ_{aq} , which equal to the summation of the whole contributions fluxes Φ_{1q} , Φ_{2q}, Φ_{3q}, Φ_{4q} times two, and also the q-axis armature reactance.It is found from table two that the d-axis reactance X_q in case of the machine with structure iron(i.e.it has a ground leakage flux) are much lower than that without structure iron (i.e. it has not ground leakage flux).

5-CONCLUSION

The magnetic equivalent circuit is easy to apply and opens the way for the per - formance estimation to be made by hand . This is extremely useful during the initial stages

	IDEAL CASE no structural iron	PRACTICAL CASE with structural iron
Permeance x 10^{-7}	S_1 = 5.213 S_2 = 13.419 S_3 = 0.933 S_4 = 0.825 S_5 = 0.000 S_6 = 3.301	S_1 = 5.213 S_2 = 13.419 S_3 = 0.933 S_4 = 0.825 S_5 = 2.815 S_6 = 6.116
Fluxes x 10^{-7} Wb	ϕ_1 = 423.7 ϕ_2 = 251.2 ϕ_3 = 110.8 ϕ_4 = 30.9	ϕ_1 = 434.4 ϕ_2 = 223.7 ϕ_3 = 103.9 ϕ_4 = 27.5
Pole potential F_p, AT	18.72	16.67
Leakage factor ϕ_1 / ϕ_2	1.687	1.942
Induced emf at 50Hz rms per 1 A exc.	4.46 (4.5)	3.97 (4)
Track pole flux denisty at 20 A exc. Tesla	1.271	1.303

Table 1 : Analysis of magnetizing fields for 100 AT excitation .

	DIRECT AXIS		QUADRATURE AXIS	
	without structure iron	with structure iron	without structure iron	with structure iron
Permeance x 10^{-7}	S_1 = 5.213 S_2 = 13.934 S_3 = 0.933 S_6 = 3.301	S_1 = 2.979 S_2 = 5.821 S_3 = 1.029 S_6 = 6.116	flux contributions	
fluxes x 10^{-7} Wb	ϕ_1 = 286.034 ϕ_2 = 518.3 ϕ_3 = 5 1.2 ϕ_4 = 181.13	ϕ_1 = 100.12 ϕ_2 = 340.3 ϕ_3 = 34.58 ϕ_4 = 205.56	ϕ_1 = 199.10 ϕ_2 = 55.40 ϕ_3 = 48.23 ϕ_4 = 17.37	ϕ_1 = 97.50 ϕ_2 = 49.36 ϕ_3 = 23.14 ϕ_4 = 4.00
F_o mmf, AT	92.07	92.07		
Pole potential (AT)	54.87	33.61		
Armature flux x 10^{-7}	518.3	340.3	640.2	348.0
Induced emf for 100 AT rms (V)	5.432	2.972	6.347	2.99
Phase cur. for 100 AT rms (A)	0.415	0.574	0.415	0.574
Reactance Ohm	13.105	5.18	15.31	5.21

Table 2 : Reactance calculations for armature excitation mmf at 100 AT .

of design since, the effect of changing a parameter or dimension can be evaluated quickly. The leakage flux has a large bearing on performance and accurate assessment of leakage is essential. It has also been demonstrated that a value of leakage factor higher than 1.4 is undesriable in view of thickness of armature core required.

It can also be concluded, from the given numerical example, that the centre air-gap reluctance is increased as the active core width is reduced. This increases both the excitation needed and leakage factor. Also that of the outer air-gap is the larger of the two reluctances in the main flux path. This air-gap is the main factor in determining the short circuit ratio of the motor which may be increased by reducing the width of outer side limbs of the armature core.

REFERENCES

[1] Levi, E. " High speed iron synchronous operating linear motors " I.E.E. conference publication on linear electric machines NO. 120, Oct. 1974

[2] Wiseman , R.W. " Graphical determination of magnetic fields " Trans. AIEE, Vol 4, No. 2 , pp141-154 Feb. 1972

[3] Eastham,J.F. " Iron-cored linear synchronous machines " Electronic and power, IEE., Vol.23, 1977, pp 239-242

[4] Eastham, J.F. and Balchin, M.J. " Characterstics of a heteropolar linear synchronous machines with passive secondary " IEE., Vol 2, No.6 , Dec.1979, pp 213-218

[5] Liwschitz Garik, and Whipple,C.C. " Electric Machinery " Vol. 2, Van Nostrand

APPENDIX:

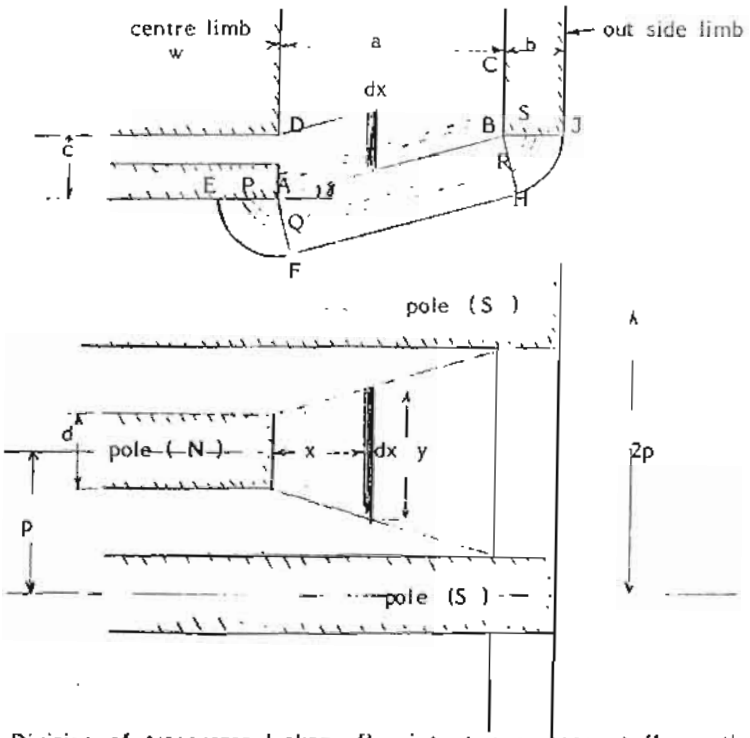

Division of transverse leakage flux into two component flux paths

For block ABCD :

Reluctance of element dx is $dR_{ABCD} = \frac{1}{\mu_o} \cdot \frac{dx \cdot \sec\gamma}{yc}$

From the lower diagram :

$$y = d + \frac{2(p-d) \cdot x}{a}$$

Then ,

$$dR_{ABCD} = \frac{1}{\mu_o} \cdot \frac{a \sec\gamma}{2c \cdot (p-d)} \quad \frac{dy}{y}$$

And , $R_{ABCD} = \int_{y=d}^{y=2p-d} dR_{ABCD} = \frac{1}{\mu_o} \cdot \frac{a \cdot \sec\gamma}{2c \cdot (p-d)} \cdot \ln\left[\frac{2p}{d} - 1\right]$

Where, $\sec\gamma = \sqrt{a^2 + c^2} / a$

$$R_{ABCD} = \frac{1}{\mu_o} \cdot \frac{\sqrt{a^2 + c^2}}{2c \cdot (p-d)} \cdot \ln\left[\frac{2p}{d} - 1\right]$$

$$S_{ABCD} = \frac{1}{R_{ABCD}} = \frac{\mu_o \cdot 2c\,(p-d)}{\sqrt{a^2 + c^2}} / \ln\left(\frac{2p}{d} - 1\right)$$

For region EFHJBA assume plane AF has axial length, d and plane BH has axial length of 2p-d. Reluctance of element QR is calculated as above

$$dR_{QR} = \frac{1}{\mu_o} \cdot \frac{\sqrt{a^2 + c^2}}{2 \cdot (p-d)} \ln\left[\frac{2p}{d} - 1\right] \cdot \frac{1}{dr}$$

Reluctance of element PQ

$$dR_{PQ} = \frac{1}{\mu_o} \cdot \frac{((\pi/2) + \gamma)}{d} \cdot \frac{r}{dr}$$

Similarly,

$$dR_{RS} = \frac{1}{\mu_o} \cdot \frac{((\pi/2) - \gamma)}{(2p - d)} \cdot \frac{r}{dr}$$

Hence whole tube of flux is associated with reluctance.

$$dR_{PQRS} = dR_{QR} + dR_{PQ} + dR_{RS}$$

$$= \frac{1}{\mu_o}\left[\frac{\sqrt{a^2 + c^2}}{2(p - d)} \cdot \ln\left(\frac{2p}{d} - 1\right) + \frac{((\pi/2) + \gamma)\, r}{d} + \frac{((\pi/2) - \gamma)\, r}{2F - d}\right] \frac{1}{dr}$$

$$dR_{PQRS} = \frac{1}{\mu_o \cdot dr} \cdot [B + Ar]$$

Where A, B are the coefficients of the polynominal in r. The permeances of region EFHJBA is the sum of all elemental permeances in parallel.

$$S_{EFHJBA} = \int_{r=o}^{r=b} (1 / dR_{PQRS})$$

$$= \frac{\mu_o}{A} \cdot \ln \frac{(Ab + B)}{B}$$

$$S_{EFHJBA} = \frac{\mu_o}{A} \cdot \ln \left[1 + \frac{Ab}{B}\right]$$

With block ABCD in parallel the net leakage path permeance is

$$S_3 = S_{EFHJBA} + S_{ABCD}$$

$$= \frac{\mu_o}{A} \ln \left(1 + \frac{Ab}{B}\right) + \frac{2c\,(p-d)\,\mu_o}{\sqrt{a^2 + c^2}} / \ln \left(\frac{2p}{d} - 1\right)$$

$$S_3 = \mu_o \left[\frac{1}{A} \cdot \ln \left(1 + \frac{Ab}{B}\right) + \frac{c}{B}\right]$$

Where, $B = \frac{\sqrt{a^2 + c^2}}{2 \cdot (p-d)} \cdot \ln \left(\frac{2p}{d} - 1\right)$

$$A = \left(\frac{\pi}{2} + \gamma\right) / d + \left(\frac{\pi}{2} - \gamma\right) / (2p - d)$$

$$\gamma = \tan^{-1} (c/a)$$